ICRC 2001

Application of fractal and wavelet analysis to Cherenkov images of the Whipple Telescope

A. Haungs[1,2]**, J. Knapp**[2]**, I. Bond**[2]**, and R. Pallassini**[2]

[1]Institut für Kernphysik, Forschungszentrum Karlsruhe, 76021 Karlsruhe, Germany
[2]Department of Physics and Astronomy, University of Leeds, Leeds LS2 9JT, UK

Abstract. Multifractal and wavelet methods are mathematical tools used in pattern recognition and image parameterisation. Their application to images of Cerenkov light from air showers as obtained in the high-resolution camera of the Whipple telescope promises improved gamma/hadron separation over the whole energy range of interest. Using recent data of on/off-source measurements for the Crab nebula and Mrk421 the performance of fractal and wavelet parameters are tested and compared with that of the conventional Hillas parameterisation. The new parameters are independent of the image orientation and depend only on the shape, i.e. on the density distribution, of the image. Hence the methods are of special interest for the search of faint, extended, or diffuse sources of TeV gamma emission. The benefit of fractal and wavelet analyses to Cherenkov image analysis is discussed for the Whipple telescope as well as for an array of telescopes like VERITAS.

1 Introduction

One of the main aims of experiments measuring high-energy cosmic γ-rays using the atmospheric Cherenkov imaging technique is the reconstruction of the energy spectrum of galactic or extragalactic sources. Starting from the raw data several steps are needed to evaluate the spectrum, all depending more or less on Monte Carlo simulations. Strongly model dependent are the selection of γ induced images, the estimation of the telescopes collecting area, and the energy reconstruction (see e.g. Mohanty et al., 1998). Hence it is important to check each step either with different Monte Carlo calculations and/or an independent methodological approach.

In this paper we compare the standard image parameterisation (for γ-selection) in terms of first and second-order moments resulting in the so-called Hillas parameters (Hillas, 1985) with a fractal and wavelet based parameterisation method (Haungs et al., 1999). The latter one uses tools well known

Correspondence to: A. Haungs (haungs@ik3.fzk.de)

from image or pattern recognition applications and is based on the idea that γ-induced Cherenkov light produces a different image than hadron-induced Cherenkov light. In parallel we compare two different Monte Carlo packages for the simulation of the air shower cascades: The KASCADE system (Kertzman and Sembroski, 1994) and the CORSIKA program (Heck et al., 1998).

2 Data and simulation base

The following investigation uses a part of the Whipple observatory database on the Crab Nebula recorded with a focal plane detector (Finley et al., 1999) consisting of 379 densely packed 1/2" photomultiplier tubes (PMT) in an inner region and 111 1" tubes in three outer rings (Fig. 1). For the present analysis only the inner PMTs are used. Data of 6 hours of
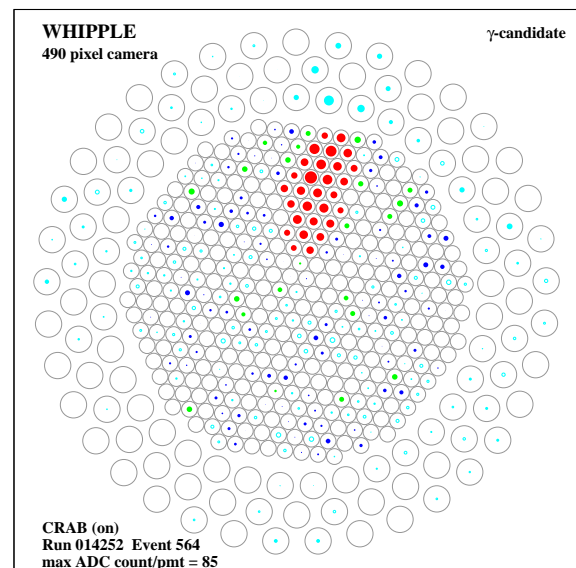
Fig. 1. Example of an recorded Whipple image with the 490 pixel camera, most probable a photon induced event.

on/off Crab observations and of 4 hours on-source measurements of Mrk 421 from the January 2001 flare are analysed. The raw data are calibrated and the ADC values of each pixel for each event are stored for the subsequent image parameterisation.

CORSIKA shower development were performed for primary photons in the energy range of 50 GeV to 30 TeV with a power law (slope of -2.6) energy dependence. High-energy hadronic interactions are simulated with the QGSJET option (Kalmykov et al., 1997). Cherenkov photons reaching the observation level are stored for fifteen virtual Whipple telescopes arranged on a 5×3 rectangular grid with $80/2\,\mathrm{m}$ and $80\sqrt{3/4}\,\mathrm{m}$ spacing, such that some of the telescopes form the planned VERITAS configuration. The position of the shower core is scattered from event to event within the telescope array resulting in a uniform core distance distribution up to 80 m and with maximum impact points of up to 180 m. A detailed simulation of the mirror and camera response is performed, including wavelength-dependent light absorption within the atmosphere, mirror reflectivity and quantum efficiency of the PMTs. Noise and night sky background (NSB) are added to each pixel according to measured distributions, i.e. with an asymmetric tail to large ADC values, which can be described, e.g., by a double Gaussian function.

The same NSB was added to a set of Cherenkov images (in photoelectrons/pixel) which were generated by KASCADE simulations, also including a detector response function. This set (provided by Vassiliev, 2001) comprises γ-induced events with fixed energies from 178 GeV to 31 TeV distributed over core distances up to 200 m. The abundances within individual energy bins follow a power law with index ≈ -2.5. More than half a million simulated images are at disposal for further investigations. Both, data and simulated showers are selected for zenith angles of about $20°$.

3   Image parameterisation

In addition to the standard parameterisation in terms of first and second order moments, resulting in the well known Hillas parameters, each simulated and recorded image is parameterised in terms of fractal and wavelet moments. The aim is to quantify hidden characteristic structures of the density distributions of the images, invisible by second-order moments but revealed by viewing the image on different scale-lengths. The mathematical procedures described in (Haungs et al., 1999) are applied to the innermost 320 pixels of the camera. Whereas for the Hillas parameterisation only pixels with a signal $\geq 4.25\sigma$ of the NSB (or $\geq 2.25\sigma$ of the NSB if there is a signal in neighbouring pixels) the fractal analysis takes all pixels into account which, after subtraction of the pedestals, have a positive signal. The *size* of an image is defined as the sum of the ADC counts of all pixels used for the Hillas parameterisation.

Fractals: Fractals are structures which display a self-similar behaviour, and the fractal nature of an object is quantified by its fractal dimension. We have calculated multifractal (and
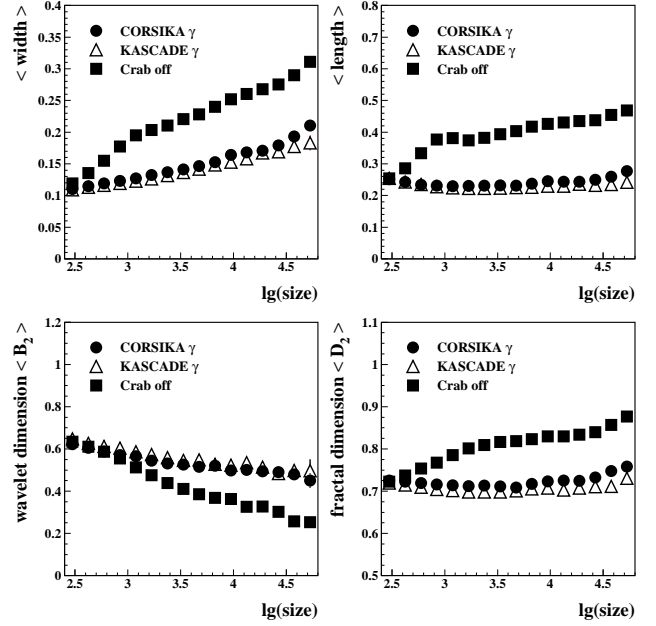
Fig. 2. Mean values of various image parameters vs. the image size in ADC counts for two different simulation programs and for Crab off-source data.

wavelet) moments of each image by dividing the image into $M = 8, 10, 20, 80$, and 320 equally sized, non overlapping parts and by calculating the sum k of ADC counts in each part. The fractal scale-length ν is defined by $\nu = \log_2 M$. The multifractal moments of order q are computed by the following expression $G_q(M) = \sum_{j=1}^{M}(k_j/N)^q$, where N is the total number of ADC counts in the image, k_j is the counts in the jth cell and $q = 2, 3, 4, 5, 6$. If the fractal moments G_q show a power law relation to the parameter M, i.e. $G_q \propto M^{\tau_q}$, then the Cherenkov images exhibit a self-similar structure, i.e. they are fractals. The exponent τ_q is determined from G_q by using the formula $\tau_q = \frac{1}{\ln 2}\frac{d\ln G_q}{d\nu}$. This exponent τ_q is related to the generalized multifractal dimension, D_q, by $D_q = \tau_q/(q-1)$. Using the total signal of each pixel including the NSB, even small images behave like fractals, moreover, an image containing only noise can be regarded as an ideal fractal as it contains only Gaussian or Poissonian parts.

Wavelets: A pattern analysis in terms of wavelets can be regarded as a sequence of filtering processes to examine the presence of local structures on different scale-lengths. When applied to the images, the wavelet moment W_q is calculated, given by: $W_q(M) = \sum_{j=1}^{M-1}(\frac{|k_{j+1}-k_j|}{N})^q$; k_j denotes the ADC count in the jth cell on a particular scale. The wavelet moment is a measure of differences of signals from one scale to the next. Again, a proportionality $W_q \propto M^{\beta_q}$ holds. The slope β of the best-fit regression line to the function $\log W_q$ vs. $\log M$ leads to the wavelet dimension $B_q = \beta_q/(q-1)$ of order q. The wavelet dimensions are sensitive to differences in the average counts in neighboring pixels on different length scales. With vanishing differences β gets smaller.

Photon induced images are more compact and have a smoother change of content from pixel to pixel. Hadron induced images are more jagged, leading to smaller wavelet dimensions and larger fractal dimensions (Fig. 2).

4 Correlations of the parameters

Investigations of the correlations between the different parameters can be used as a measure for their sensitivity, i.e. a measure for the gain on γ/hadron separation by the new parameters. The correlation coefficient c between two variables x and y, is defined as

$c = \sum_{i=1}^{n}(x_i - \overline{x})(y_i - \overline{y}) / \sqrt{(\sum_{i=1}^{n}(x_i - \overline{x})^2)(\sum_{i=1}^{n}(y_i - \overline{y})^2)}$

and is a measure of the linear association between the two variables. $c \equiv \pm 1$ means a perfect, positive or negative, correlation between x and y, and $c \equiv 0$ means no correlation at all. The four image shape parameters in Table 1 are correlated to each other with roughly the same strength, and the coefficients are clearly < 1. Hence we expect on average a gain in γ/hadron separation sensitivity with the new observables, especially wavelet parameters correlate least with width and length. The correlation between fractal and wavelet parameters of different q are larger than those shown in Tab. 1, but lowest for B_2 with B_6 and D_2 with D_6, respectively. Therefore we use B_2, B_6, D_2, and D_6, to examine the structure of the Cherenkov images. It is important to note the low correlation of all shape parameters with the size of the image, which entails a uniform efficiency over the whole energy range if selection cuts are applied.

Table 1. Correlation coefficients for image parameters calculated with the whole set of simulations. Below the diagonal are the values for the KASCADE simulations, above those for CORSIKA generated showers.

	Width	Length	D_6	B_6	Size
Width		0.807	0.840	0.707	0.339
Length	0.802		0.836	0.747	0.199
D_6	0.843	0.816		0.878	0.224
B_6	0.705	0.718	0.870		0.148
Size	0.290	0.168	0.199	0.135	

5 Comparisons of the Monte Carlo models

In general the images for primary photons agree very well between the two different Monte Carlo models. Fig. 2 and Table 1 show that, for a given size, the image parameters differ only slightly. But there are differences in the lateral distribution of the Cherenkov photons: CORSIKA produces a few more photons than the KASCADE model (Fig. 3). Furthermore CORSIKA has larger fluctuations in the size distribution from shower to shower displayed in Fig. 3 (right panel). Hence the simulated size-to-energy relation, which is an important factor for the energy reconstruction, seems to
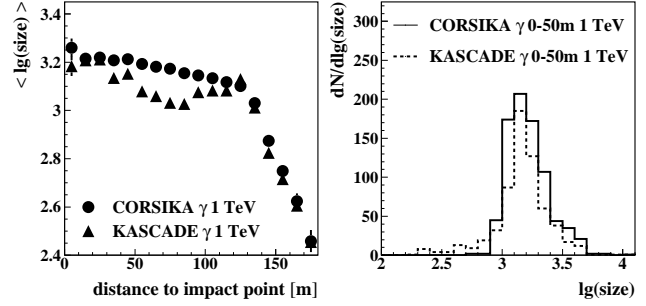
Fig. 3. Comparison of the size distributions of CORSIKA and KASCADE for fixed primary energy. Left: size as function of core distance; right: size distribution for a range of core distances.

be more sensitive to differences of Monte Carlo generators than the parameterisation of the image shapes.

6 Quality of γ/hadron separation

The quality of the γ/hadron separation achieved with different image parameters is estimated by looking at the significance of the photon excess of the standard γ-source, the Crab Nebula. After some general cuts (i.e. that the Hillas parameterisation was successful and the pixel with the largest ADC count is not at the edge of the inner field of PMTs) the significance is calculated from the number of excess events in the range of the orientation parameter $\alpha < 15°$, according to the likelihood ratio method described by Li and Ma, (1983). Without any further cuts the significance of the on/off data used is determined to be 3.9σ. The standard cuts of the Whipple Collaboration (Mohanty et al., 1998), the so-called supercuts, lead for the same data set to a significance of 10.7σ, but with the relatively small number of 346 excess events. These supercuts use the fact that the photons are coming directly from the source (shape and orientation parameters). For the detection of extended or diffuse sources only shape parameters can be used. Here the new observables which are pure shape parameters allow for improvement. To check this, the standard cuts were weakened and only the shape parameters width and length have been used, resulting
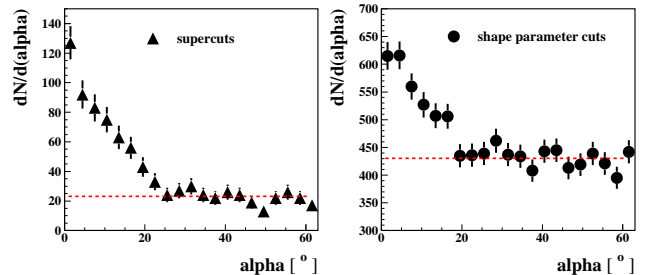
Fig. 4. Distribution of the α parameter for the Mrk421 data after cut on the shape parameters (width, length, D_2, D_6, B_2, and B_6) and after the Whipple standard cuts.

in 6.6σ, with 549 excess events. This can be compared with 5.1σ, with 763 excess events, obtained by cuts on the fractal parameters, only. These cuts on D_6, D_2, B_6, and B_2 have been optimized by comparing the simulated distributions for γ with the Crab off-source data. The fractal and the weakened Hillas cuts together (only shape parameters) result in a significance of 7.5σ, with 489 excess events, clearly improving the performance over both sets of cuts alone. The combined shape cuts were also applied to Mrk421 on-source data. Fig. 4 shows the α-distribution after this selection and after the supercuts. For the shape cuts the background remains larger but also the γ selection efficiency is increased.

7 Neural net investigations

The correlation between the parameters are not strictly linear and also have a varying dependence on the size. Therefore, linear cuts might not be the best way for the γ-selection. A multivariate non-parametric classifying method seems a better choice. To investigate this we use an artificial neural network tool (Lönnblad et al., 1994) with five input observables: width, length, D_2, B_2, and the size. We restrict the events to sizes > 500 to be far away from threshold problems (see also Fig. 2). The net is trained with the CORSIKA γ-sample for an output value of zero and the Crab off-source data (for 1 as output). After optimizing the net parameters the network-classification is applied to Crab and Mrk421 on-source data. Fig. 5 shows the distribution of the net output values after adjusting the network and the resulting α-distributions for events with a network output value of < 0.15. The significance of the γ selection for the Crab on/off data is 9.5σ. It should be noted that again only shape parameters are used and the significance reached after the neural network application is better than with linear cuts on the same parameters. The net is trained with Crab off-data. Though the result for the AGN data is very promising, we expect a bias for the application of the trained network to Mrk data. For a detailed investigation with the presented method off-data of the corresponding region of the sky should be used.

8 Implications for a telescope array

For forthcoming experiments which use telescope arrays, it is important how the image parameters work if several images of the same shower are available. The simplest ansatz is to average the parameters and take the mean value. This is done for the CORSIKA showers using telescope positions of VERITAS. On average 6 to 7 images with successful parameterisation are available for each γ event. Fig. 6 compares the mean values with the distributions of single telescope measurements for the width and one of the fractal parameters. The distributions get narrower for all parameters, especially for the new parameters which indicates a very welcome robustness of this analyses technique. Thus, with a given impact point an improved γ/hadron separation can be achieved,

even in this simplest case of multi-telescope analysis. Certainly more sophisticated methods can be developed.
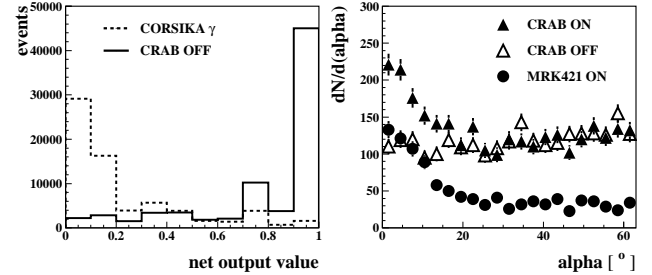
Fig. 5. Left: output of the neural network after training. Right: α distribution of Crab on/off and Mrk421 on-source data after a cut on the neural network output value < 0.15.
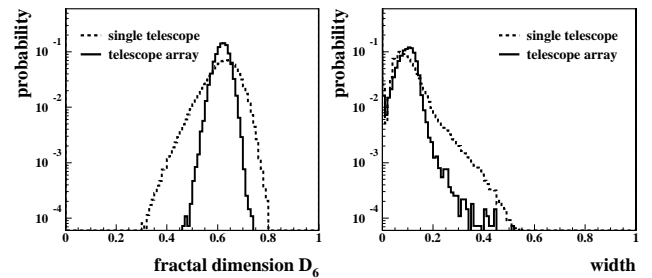
Fig. 6. Probability distribution of two image parameters for a single telescope and the mean value over an array of 7 telescopes.

9 Summary

Whipple images can be parameterised by fractal and wavelet methods. The parameters presented here contain complementary information to the well-known Hillas parameters. They are only shape dependent, i.e. can be used for the search of extended or diffuse sources. Non-parametric methods like artificial neural networks can improve the γ/hadron separation efficiency.

References

Finley, J.P., et al., Proc. *Towards a Major Atmospheric Cherenkov Detector VI*, AIP Conf.Proc. 515, 301, 1999.
Haungs, A., et al., Astrop.Phys., 12, 145, 1999.
Heck, D., et al., FZKA 6019, Forschungszentrum Karlsruhe, 1998.
Hillas, A.M., Proc. 19th ICRC, La Jolla, Vol.3, 445, 1985.
Kalmykov, N., et al., Nucl. Phys. B (Proc. Suppl.), 52B, 17, 1997.
Kertzman, M.P. and Sembroski, G.H., NIM A, 343, 629, 1994.
Li, T.P. and Ma, Y.Q., Astrop.J., 272, 317, 1983.
Lönnblad, L., et al., CERN Preprint, CERN-TH. 7135/94, 1994.
Mohanty, G., et al., Astrop.Phys., 9, 15, 1998.
Vassiliev, V., private communication, 2001.